Journal of Magnetism and Magnetic Materials 377 (2015) 446–451

Contents lists available at ScienceDirect

Journal of Magnetism and Magnetic Materials

journal homepage: www.elsevier.com/locate/jmmm

An integrated device for magnetically-driven drug release and *in situ* quantitative measurements: Design, fabrication and testing

I.J. Bruvera [a], R. Hernández [b], C. Mijangos [b], G.F. Goya [a,c,*]

[a] Aragon Institute of Nanoscience (INA), University of Zaragoza, 50018, Spain
[b] Instituto de Ciencia y Tecnología de Polímeros, CSIC, Juan Cierva 3, E-28006 Madrid, Spain
[c] Condensed Matter Physics Department, Science Faculty, University of Zaragoza, 50009, Spain

ARTICLE INFO

Article history:
Received 16 June 2014
Received in revised form
11 September 2014
Accepted 27 October 2014
Available online 6 November 2014

Keywords:
Drug release
Magnetic nanoparticles
Magnetic hyperthermia
Hydrogels

ABSTRACT

We have developed a device capable of remote triggering and *in situ* quantification of therapeutic drugs, based on magnetically-responsive hydrogels of poly (*N*-isopropylacrylamide) and alginate (PNiPAAm). The heating efficiency of these hydrogels measured by their specific power absorption (SPA) values showed that the values between 100 and 300 W/g of the material were high enough to reach the lower critical solution temperature (LCST) of the polymeric matrix within few minutes. The drug release through application of AC magnetic fields could be controlled by time-modulated field pulses in order to deliver the desired amount of drug. Using B12 vitamin as a concept drug, the device was calibrated to measure amounts of drug released as small as $25(2) \times 10^{-9}$ g, demonstrating the potential of this device for very precise quantitative control of drug release.

1. Introduction

Magnetic controlled drug delivery is based on the employment of a magnetic field to trigger on-demand drug release employing magnetic nanoparticles (MNPs) as heating agents [1]. The ability of generating heat on the MNPs is measured by the specific power absorption (SPA), which is the power absorbed per unit mass of magnetic nanoparticles [2,3]. The physical mechanisms of heat generation of the single-domain MNPs under an AC field were first studied by Hergt et al. [4] Some years later, a simple model was developed by Rosensweig [5] based on the magnetic and rotational relaxation for the specific case of single domain magnetic particles dispersed in a liquid matrix. This and other subsequent theoretical models have successfully explained the physical mechanisms by which the energy of the alternating magnetic field is absorbed by an assembly of single-domain MNPs [5–8]. At the frequencies involved in our experiments the power absorption can be described through the relaxation of the magnetic moment induced by thermal fluctuations, known as the Neel–Brown relaxation process. The SPA values expected for single domain MNPs of a given material (*i.e.*, a specific magnetic anisotropy) is known to depend strongly on the average particle size as well as the size distribution [9]. In the specific case of Fe_3O_4 magnetic cores, the maximum SPA have been reported to be around particle sizes of ≈ 30 nm [10].

To date, a number of magnetic controlled released materials for drug delivery have been reported, many of which are based on the incorporation of magnetic iron oxide nanoparticles on thermo-sensitive polymer hydrogels to give rise to polymer ferrogels. As depicted in Fig. 1, an alternating current (AC) magnetic field can be used to trigger localized heating of a MNP-loaded hydrogel, inducing a volume change in the host polymer matrix and allows diffusion and release of drugs [11–14].

Among thermo-sensitive hydrogels, hydrogels based on poly (N-isopropyl acrylamide) (PNiPAAm) and related copolymers are one of the most studied for biomedical applications. PNiPAAm contains hydrophobic groups that provide a lower critical solution temperature (LCST) of ~32 °C in water. At room temperature PNiPAAm is relatively hydrophilic and can be highly swollen. When heated above a critical temperature, the PNiPAAm becomes relatively hydrophobic, so the hydrogel collapse [15,16]. In magnetically-loaded PNiPAAm, the temperature rise is obtained, by power absorption of the embedded MNPs, from an externally applied AC field [17].

One of the drawbacks in the employment of PNiPAAm gels for controlled drug release is the slow response to temperature changes which restricts wider applications, such as on–off valves, artificial muscles or drug delivery applications [18]. One strategy to overcome this drawback is the combination of crosslinked PNiPAAm with a natural polymer such as alginate in the form of a semi-interpenetrating polymer network. The resulting material

* Corresponding author at: Aragon Institute of Nanoscience (INA), University of Zaragoza, 50018, Spain. Fax: +34 976762776.
E-mail address: goya@unizar.es (G.F. Goya).

http://dx.doi.org/10.1016/j.jmmm.2014.10.149
0304-8853/

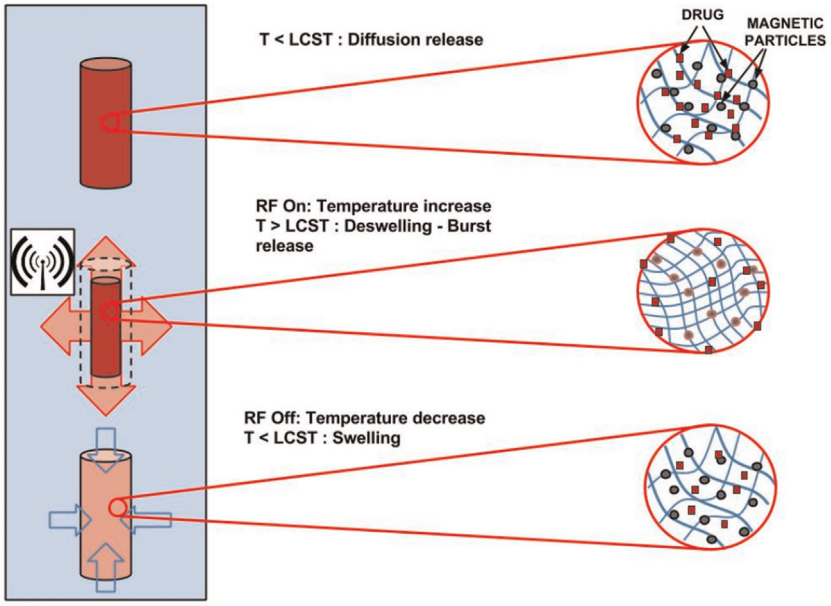

Fig. 1. Schematic drawing of the ON–OFF cycles and their effect on the thermoresponsive nanocomposites of PNiPAAm. The ac magnetic field triggers the heating and drug burst release by the contraction of the ferrogel network when crossing the LCST (lower critical solution temperature).

presents an increased dwelling rate with respect to raw poly(NIPAAm), due to an increased porosity promoted during the reaction of crosslinking of the N-isopropylacrylamide monomer in the presence of alginate [19]. The presence of alginate allows for the *in situ* synthesis of iron oxide MNPs due to the fact that the carboxylic groups in alginate can bind to iron cations [20].

In this work, a proof-of-concept device was designed and constructed in order to test the validity of magnetically loaded semi-interpenetrating polymer networks of alginate and PNiPAAm as materials for magnetically controlled drug release. The device was capable to control the amount of a model drug released (vitamin B12) through a time-controlled magnetic pulse and, after proper calibration, to quantify released vitamin B12 amounts as small as 25(2) ng.

2. Materials and methods

2.1. Materials

The N-Isopropylacrylamide (N-AAm) (Panreac), the initiator potassium persulfate (Fluka), the crosslinker *N*, *N*′-Methylenebisacrylamide (Bis) (Aldrich), and the accelerator *N*,*N*,*N*′,*N*′-Tetramethylethylenediamine (TEMED) (Bio-Rad) were used as received. Alginic acid sodium salt from brown algae with a 65–70% guluronnic acid and M_w=100–200 kDa according to the manufacturer was purchased from Aldrich and used as received. Alginate stock solutions were prepared by dissolving alginate powder in distilled water to yield 1 g/100 mL solutions. Ferrous chloride ($FeCl_2 \cdot 4H_20$), ferric chloride ($FeCl_3 \cdot 6H_20$) and vitamin B12 were purchased from Aldrich and used as received.

2.2. Preparation and chemical characterization of ferrogels

Semi-interpenetrating (semi-IPN) polymer networks constituted by alginate and PNiPAAm (Alg-PNiPAAm) were obtained by polymerizing 3 g of N-AAm and 0.15 g of Bis in 40 mL of an 1 wt% alginate aqueous solution. Solutions were poured out into Teflon molds having 8 mm diameter and 40 mm lenght and allowed to react at room temperature for 24 h. Samples obtained were dialyzed against fresh water during 2 days to remove all the unreacted monomer.

For the in situ synthesis of iron oxide MNPs, Alg-PNiPAAm samples were immersed in 200 mL aqueous solution containing 2.1 g $FeCL_2 \cdot 4H_2O$ and 5.8 g $FeCl_3 \cdot H_2O$ under constant N_2 bubbling during 4 h. After that period of time, yellowish gels were obtained that were immersed in a 0.5 M NH_3 (30 wt%) under constant N_2 bubbling during 30 min. The resulting black Alg-PNiPAAm ferrogels were washed with distilled water for 24 h. The procedure of oxidation was repeated three times. Thermogravimetric measurements were performed on dried gels on a Q500 TA Instruments TGA, using a nitrogen stream as the purge gas, at a heating rate of 10 °C/min over the range 40–900 °C. The residual weight obtained at 900 °C obtained for Alg-PNiPAAm ferrogels can be taken as an indication of the iron oxide content in the samples. The total water content, W_t, was calculated from the mass of the hydrated (m_s) and dried (m_{dry}) gels through

$$W_t = \frac{m_s - m_{dry}}{m_{dry}}$$

The iron oxide content determined through TGA measurements was 22 wt% and the water content was found to be 90 wt%. The particle $<d>$ size of the iron oxide MNPs was found to be $<d>$ =20 nm as determined through transmission electron microscopy combined with small angle-X-ray measurements [21].

2.3. Magnetic characterization of the ferrogels

Magnetization *vs.* field curves $M(H)$ were performed on a previously dried fraction of the ferrogel having mass 6.5(1) mg, and a control sample (*i.e.* without MNPs) of dry mass 14.2(1) mg. The control sample measurement was used to identify the diamagnetic contribution of the hydrogel matrix. Measurements were performed on a Vibrating Sample Magnetometer (LakeShore 7304) in fields up to H=1.5 MA/m at room temperature. Specific power absorption (SPA) measurements were done using a commercial induction heating station (EasyHeat, Ambrell) working at f=360 kHz and field amplitudes up to H=45 kA/m. The working space was conditioned with an adiabatic sample holder for a measuring volume up to 500 μl. The temperature was measured

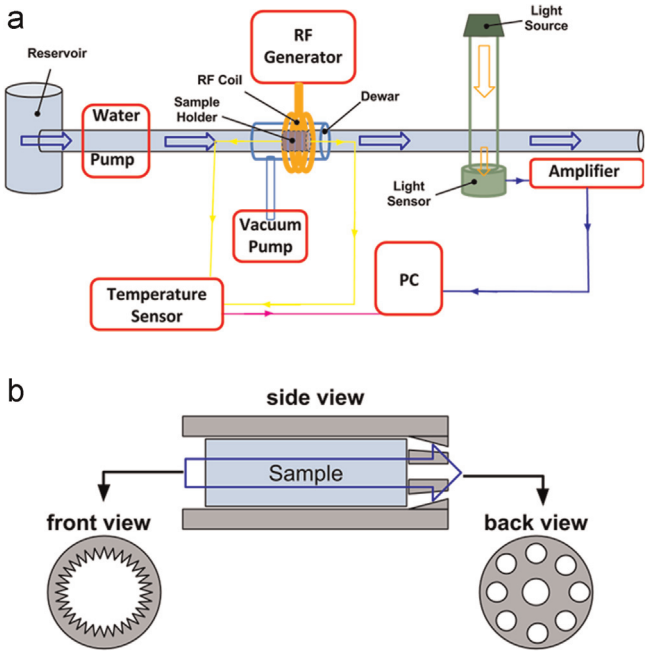

Fig. 2. Device drawing. a: open circuit including detection photometer and magnetic field applicator. b: detail of the sample holder. Water enters the chamber from the left side and circulates around the sample through the small channels on the walls.

Fig. 3. Top view of a section of the device. *A*=RF coil, *B*=Dewar, and *C*=Sample holder.

using an optic fiber probe (Reflex, Neoptix) immune to radio frequency environments.

The specific power absorption (SPA) of the ferrogel was determined by the SPA of the constituent MNPs incorporated into the gels. Therefore we measured the heating efficiency of the pure colloids from the temperature increase (ΔT) of a given mass of nanoparticles (m_{NP}) diluted in a total mass of liquid carrier (m_{LIQ}) under the application of the magnetic field through

$$SPA = \frac{c_{liq}\ m_{liq}}{m_{NP}}\left(\frac{\Delta T}{\Delta t}\right)$$

where C is the heat capacity of the sample and $\Delta T/\Delta t$ the initial slope of the temperature versus time heating curve. All experiments were done after a waiting time of 60–120 s with the magnetic field off, to allow thermalization of the samples.

2.4. Design and construction of the device for measuring magnetic-controlled release

A schematic drawing of the device is shown in Fig. 2a. The sample space is located in the center of a 5-turn solenoid that applies the current to generate the AC field. The sample place is connected to a water circuit, with a peristaltic pump as flow propellant. The water circuit contains also a reservoir and a sample holder section (which is surrounded by the Dewar chamber and the RF coil) and the last section goes through a homemade photometer composed by two photodiodes centered at the wavelengths of maximum absorbance of the specific drug (vitamin B12) used here. At the sample space, the water circuit can be opened for hydrating and loading the samples.

The water circuit is composed of a water reservoir from which the circulating water is extracted and passed through the sample holder. Sample position was centered at the RF coil to have homogeneous (constant) B12 values along the sample. The water thus flowed through and around the sample with the calculated flow rate to avoid spurious cooling that could prevent the gel to reach the critical temperature during exposure to RF field. A fine control of the flow rate was attained by a home-made peristaltic pump (OEM component, Watson Marlow 400F/D3). The excitation RF field is generated by the same equipment used for the power dissipation measures of the samples. The water circuit goes through the coil of the applicator so the sample holder occupies the maximum field region. A detailed schematic representation of the sample holder is shown in Fig. 2b.

The heat dissipated by the circulating currents at the RF coil (I=600 A) made necessary to isolate the sample space by introducing a vacuum chamber between both elements. The glass chamber surrounded the sample holder and was connected to a vacuum turbomolecular pump working at pressures of about 10^{-7} mbar. The top view of a section of the device is shown in Fig. 3.

2.4.1. Photometer

In order to have a real time reading of the vitamin B12 concentration in the water flow, a homemade photometer was built and added to the last part of the circuit. It consists of a couple of photodiodes (Centronic BPW21) with a 600 nm low pass interference filter (Edmund Optics) placed under the water tube. The signal of the diodes is amplified and digitalized so it can be seen in real time as a voltage *vs*. time plot in a computer. A commercial halogen lamp is used as light source. The optic filter and diodes were selected so the device is sensitive to the variations in light intensity in the range 450–600 nm which contains the visible absorbance maximum of vitamin B12 (see Fig. 4a). A photometer calibration (Fig. 4b) curve was made prior to the experiments in order to obtain the values of absolute concentration of vitamin B12 from the photometer reading. It also allowed us to determine the sensibility range of our device. As a part of the calibration protocol designed for this purpose, the instrument readings started when circulating water was flowing through the closed circuit and then small volumes of a concentrated vitamin B12 solution were added at known intervals letting the readings to stabilize.

From the average value of each plateau and the corresponding calculated concentration, a calibration curve diode voltage *vs*. concentration was obtained. The data showed the expected Lambert–Beer exponential dependence between the diode voltage and

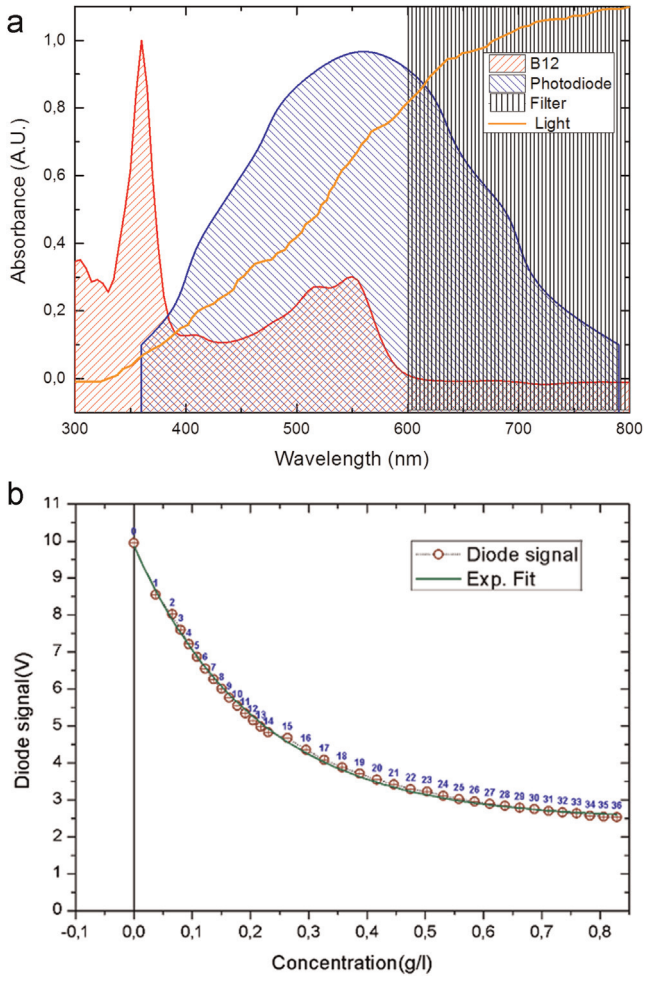

Fig. 4. (a) Absorption spectrum of B12 vitamin (red), response profile of the photodiodes (blue), emission of the lamp (orange) and cutoff of the optic filter (black). (b) Calibration curve of the photometer. Lambert–Beer exponential fit confirms the proportional relation between light intensity and diode signal. (For interpretation of the references to color in this figure legend, the reader is referred to the web version of this article.)

the vitamin B12 concentration $V(c) = Ae^{-c/\tau} + V_0$, where c is the concentration, $A+V_0$ is the signal from pure water ($c=0$) and τ is a constant containing the effects from both optical path and the molar extinction coefficient. The value $A+V_0$ depends on the light intensity emitted by the source, but τ is the same for all calibration conditions, provided the absorbent substance and the geometry of the photometer remains unaltered. As shown Fig. 4b, the good fit confirmed the linear relation between the light intensity and the photodetector signal.

Additional experiments were performed with blank (*i.e.* without MNPs) Alg-PNiPAAm hydrogels in order to test the sensitivity of the signal to variation other than the concentration of released drug (*e.g.*, external light variations, pure water circulation, bubbles, *etc.*). For this purpose, a dry sample was first hydrated in MiliQ water by putting it in the sample holder and circulating the water for 24 h. Then, the photometer was started, and 15 mg of solid B12 was added to the circuit reservoir containing 17.5 mL of MiliQ water.

Finally, the reservoir was changed for another one containing clean MiliQ water and the circuit was open so, after flowing through the photometer, the water leaved the system. In this stage the RF field was turned on for 5 minutes. The voltage readings from the diodes as a function of time for the three stages of the experiment show the response of the photometer to the change in light intensity due the variations in B12 concentration (results not shown). The system was able to detect even the bubbles circulating through the circuit. No effect of the field exposure was detected.

3. Results and discussion

3.1. Magnetic characterization of the ferrogel sample

To evaluate the Alg-PNiPAAm ferrogel as a suitable material for controlled magnetic drug delivery, its magnetic response was measured. The overall magnetic response of the thermosensitive material, through the magnetization per gram of ferrogel, is plotted in Fig. 5. The nearly zero remanent magnetization and coercive field (see inset of the Fig. 5) demonstrates that the sample is in the superparamagnetic state at room temperature, as measured by dc fields of the magnetometer.

The actual capability of the Alg-PNiPAAm ferrogel to be remotely 'activated' by an AC magnetic field was evaluated through the heating performance by measuring its specific power absorption (SPA) as a function of the applied magnetic field amplitude and frequency under static conditions (*i.e.*, without circulating water flow).

The heating response of the Alg-PNiPAAm ferrogel (shown in Fig. 6) followed approximately a quadratic H^2 dependence with applied fields up to ≈ 20 kA/m as expected from the relaxation power absorption model of single domain nanoparticles [8]. At larger field amplitudes, the SPA values are nearly constant, and this can be understood by observing that for applied fields larger than the coercivity field H_C of the MNPs at the experimental frequency (i.e., $H > H_C$ at $f=360$ kHz), the area under the $M(H)$ curve reaches its maximum value, and therefore no further increase of the work done by the systems can be expected.

3.2. Drug release experiment

Fig. 6 shows the data from the experiment of field-induced release carried out in the previously described device, on a dry sample of Alg-PNiPAAm ferrogel. The sample was introduced inside the device and rehydrated by circulating a solution of B12 (initial concentration of 1.034(5) g/L) for 24 h in closed-circuit mode. The rate of the water flowing past the sample was precisely controlled to avoid excessive refrigeration of the sample, allowing the transition temperature, LCST, to be reached. From the

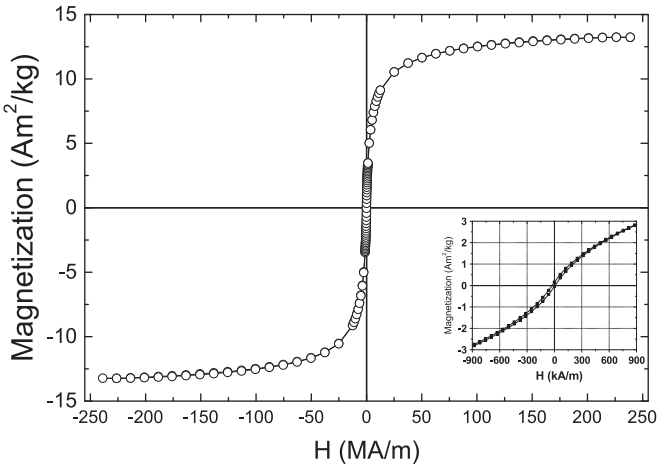

Fig. 5. Magnetization curve taken at $T=295$ K for the Alg-PNiPAAm ferrogel. Inset: Low field region showing the absence of remanence and coercive field.

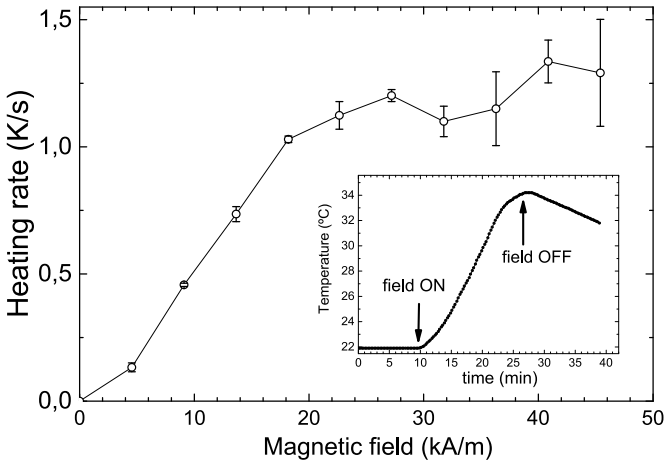

Fig. 6. Values of heating rates of the Alg-PNiPAAm ferrogel as a function of the magnetic field amplitude *H*. Inset: Typical heating curve *T vs*. time, showing the points of turning ON and OFF the AC field.

measured SPA values of the sample, a maximum allowable flow rate of $Q=0.41$ mL/s was estimated for a temperature increase of $\Delta T=1$ K for the water during the flowing past the sample. In Fig. 7A, the complete record is shown: the initial signal of 2.0 V corresponds to the circulating aqueous solution of vitamin B12 used to load the gel (time scale was restarted). Around $t=18$ min the aqueous solution of vitamin B12 is replaced by pure Milli-Q water to wash the whole device and the sample so the only vitamin B12 left is that inside the gel. After 100 min the signal was stable in the $c=0$ equivalent value. Magnification of the three liberation peaks induced by the field application is shown in Fig. 7B–D.

The quantitative estimation of drug released in each pulse can be done by integrating the area under the peaks, adequately placed at the signal level background immediately before each burst. In our system, the baseline could be clearly seen due to the small noise level along the whole experiment. From the acquired data is possible to determine the absolute mass m of B12 vitamin expelled each time. Converting the voltage values $V(t)$ to concentration $c(t)$ from the calibration curve using known concentrations of B12, the amount of B12 liberated is equal to the peak area,which can be estimated by a numerical integration and multiplied by the flow rate Q:

$$m = Q\int_{t0}^{tf} c(t)dt$$

where t_0 and t_f are determined by the time interval of each liberation event. Using this expression we estimated that the liberated amount of B12 at the first burst was $m=2.75(3)\times 10^{-10}$ g. As expected from a ferrogel response, the amount of drug released decreased after each subsequent pulse. From the third release pulse, the amount detected was $m=25(6)\times 10^{-12}$ g demonstrating the high sensitivity of the technique for detecting minute amounts of released drug.

The results presented above demonstrate the capability of this device to remotely trigger controlled amounts of specific drugs by controlling the time width of the RF pulses. Furthermore, the integration of a compact optical device allowed *in situ* measurement of minute amounts of the released drug. The control of the released drug could be achieved by additional ways, such as controlling the magnetic RF pulse frequency or amplitude, as well as the water flux rate through the sample. Further design with electronic feedback between temperature sensors and power source could allow a precise stimulus/response profiling of each thermoresponsive material to be tested. In cases where a faster release response is required, this could be achieved by increasing

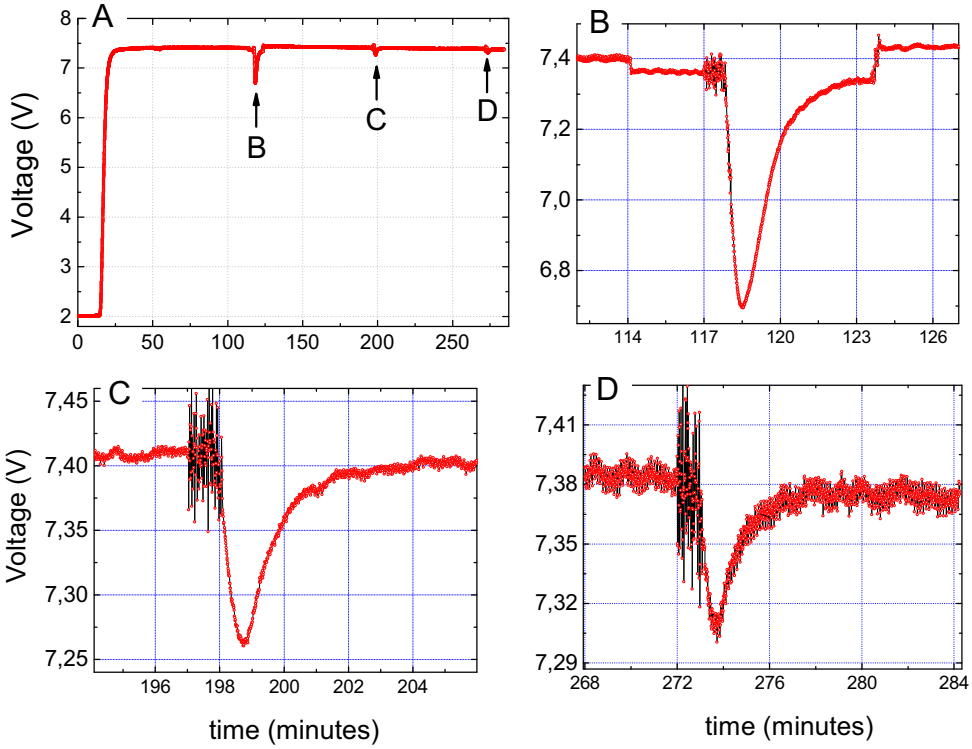

Fig. 7. Results of the magnetic field induced liberation performed on the Alg-PNiPAAm ferrogel: (A) complete experiment along 208 min. The initial signal of 2.0 V corresponds to the background B12 concentration circulating. At $t=18$ min the solution is replaced by pure MiliQ water and the signal rises to 7.4 V. (B)–(D) Expanded view of the three voltage peaks at $t=118.5$, 199 and 274 min, due to the concentration burst released by the magnetic field pulses.

the RF amplitudes or the effective SPA values of the constituent MNPs. Although the optimal measurement conditions will depend on the specific nature of the sample/drug used, it is clear that, with the possibility of varying field amplitude, flow rate and photometer sensibility, the system prototype build is robust enough to perform a wide variety of experiments keeping both the observed reproducibility and sensitivity. From the point of view of the material used (MNP-loaded polymers), the performance admits also improvements through the optimization of the SPA of individual nanoparticles for maximum heat release, as well as a maximization of the loaded amounts per gram of polymer, since the average SPA of the ferrogel (i.e., MNPs+polymer) is proportional to the concentration of the magnetic material loaded. Although it is not expected that the heating capacity of the ferrogel will depend on the concentration of loaded drug, improvements on the drug-loading capacity could also result in a more effective therapeutic performance.

One limitation of the present design that could be easily removed is related to the spectral response of the test drug: in the present experiments, the chosen B12 vitamin has a maximum absorption within the visible region due to the intensity of the main absorption peak. Current commercial spectrophotometers are capable to cover the entire UV–vis portion of the EM spectrum and thus the integration of such devices to our system will allow measuring a wide range of molecules of biological interest.

4. Conclusions

A new device has been designed, constructed and successfully tested to remotely induce drug release from a thermoresponsive material, with further *in situ* quantification of the amount of drug released. The thermoresponsive material was a ferrogel based on poly(*N*-isopropylacrylamide) and alginate mixture loaded with iron oxide magnetic nanoparticles, the latter optimized in size for maximum power absorption. The overall performance of the device is enough to detect minute concentrations of B12 released after magnetic field pulses of 60 s. This proof of performance shows the potential of the system as a therapeutic device, capable of working onto target regions at any depth of the body without affecting the surrounding healthy tissues. Although many specific clinical issues are yet to be solved, mainly about biocompatibility and implant strategies, there are already well established technologies capable to integrate the main components of the present device on a single platform, to produce a lab-on-a-chip device adequate for *in situ* therapies of remotely controlled drug release. In turn, miniaturization could allow the system to be improved by adding a feedback system to control the process by sensing the released amount of the therapeutic drug. As the applications of this strategy are only at the early stages, the technological potential of these integrated devices is yet to be discovered.

Acknowledgments

Financial support from MEC (MAT-2010-19326 and MAT 2011-24797) is gratefully acknowledged. R. Hernández thanks MEC for a Ramon y Cajal contract.

References

[1] C.S.S.R. Kumar, F. Mohammad, Magnetic nanomaterials for hyperthermia-based therapy and controlled drug delivery, Adv. Drug Deliv. Rev. 63 (9) (2011) 789–808.
[2] A. Jordan, et al., Magnetic fluid hyperthermia (MFH): Cancer treatment with AC magnetic field induced excitation of biocompatible superparamagnetic nanoparticles, J. Magn. Magn. Mater. 201 (1–3) (1999) 413–419.
[3] K. Melanie, et al., Characterization of iron oxide nanoparticles adsorbed with cisplatin for biomedical applications, Phys. Med. Biol. 54 (17) (2009) 5109.
[4] R. Hergt, et al., Physical limits of hyperthermia using magnetite fine particles, IEEE Trans. Magn. 34 (5) (1998) 3745–3754.
[5] R.E. Rosensweig, Heating magnetic fluid with alternating magnetic field, J. Magn. Magn. Mater. 252 (1–3) (2002) 370–374.
[6] J. Carrey, B. Mehdaoui, M. Respaud, Simple models for dynamic hysteresis loop calculations of magnetic single-domain nanoparticles: application to magnetic hyperthermia optimization, J. Appl. Phys. 109 (2011) 8.
[7] N.A. Usov, B.Y. Liubimov, Dynamics of magnetic nanoparticle in a viscous liquid: application to magnetic nanoparticle hyperthermia, J. Appl. Phys. 112 (2012) 2.
[8] E.T. Lima Jr., T.E. Torres, L.M. Rossi, H.R. Rechenberg, T.S. Berquo, A. Ibarra, C. Marquina, M.R. Ibarra, G.F. Goya, Size dependence of the magnetic relaxation and specific power absorption in iron oxide nanoparticles, J. Nanopart. Res. 15 (2013) 1654.
[9] E. Lima Jr., et al., Size dependence of the magnetic relaxation and specific power absorption in iron oxide nanoparticles, J. Nanopart. Res. 15 (2013) 5.
[10] M.A. Gonzalez-Fernandez, et al., Magnetic nanoparticles for power absorption: optimizing size, shape and magnetic properties, J. Solid State Chem. 182 (10) (2009) 2779–2784.
[11] D.E. Meyer, et al., Drug targeting using thermally responsive polymers and local hyperthermia, J. Control. Release 74 (1-3) (2001) 213–224.
[12] A. Baeza, et al., Magnetically triggered multidrug release by hybrid mesoporous silica nanoparticles, Chem. Mater. 24 (3) (2012) 517–524.
[13] N.S. Satarkar, J.Z. Hilt, Magnetic hydrogel nanocomposites for remote controlled pulsatile drug release, J. Control. Release 130 (3) (2008) 246–251.
[14] C. Brazel, Magnetothermally-responsive nanomaterials: combining magnetic nanostructures and thermally-sensitive polymers for triggered drug release, Pharmaceut. Res. (2009).
[15] H.G. Schild, Poly(N-isopropylacrylamide): experiment, theory and application, Prog. Polym. Sci. 17 (2) (1992) 163–249.
[16] A.S. Hoffman, Hydrogels for biomedical applications, Adv. Drug Deliv. Rev. 54 (1) (2002) 3–12.
[17] T. Hoare, et al., Magnetically triggered nanocomposite membranes: a versatile platform for triggered drug release, Nano Lett. 11 (3) (2011) 1395–1400.
[18] Y. Qiu, K. Park, Environment-sensitive hydrogels for drug delivery, Adv. Drug Deliv. Rev. 64 (Suppl.) (2012) 49–60.
[19] R. Hernández, C. Mijangos, In situ synthesis of magnetic iron oxide nanoparticles in thermally responsive alginate-poly(< I > N < /I > -isopropylacrylamide) semi-interpenetrating polymer networks, Macromol. Rapid Commun. 30 (3) (2009) 176–181.
[20] R. Hernández, J. Sacristán, C. Mijangos, Sol/gel transition of aqueous alginate solutions induced by Fe^{2+} cations, Macromol. Chem. Phys. 211 (11) (2010) 1254–1260.
[21] R. Hernández, et al., Structural organization of iron oxide nanoparticles synthesized inside hybrid polymer gels derived from alginate studied with small-angle x-ray scattering, Langmuir 25 (22) (2009) 13212–13218.